ELSEVIER

Contents lists available at ScienceDirect

Journal of Luminescence

journal homepage: http://www.elsevier.com/locate/jlumin





Temperature-dependent luminescence of CaFCl:Yb,Er upconverting nanocrystals

B. Dulani Dhanapala, Hashini N. Munasinghe, Federico A. Rabuffetti

Department of Chemistry, Wayne State University, Detroit, MI, 48202, USA

ARTICLE INFO

Keywords: CaFCl Upconverting Nanocrystals Temperature Luminescence Thermometry

ABSTRACT

CaFCl:Yb,Er upconverting nanocrystals were synthesized via solution-phase thermolysis of metal trifluoroacetates and trichloroacetic acid and their temperature-dependent luminescence was probed in the 150–450 K range. Nanocrystals exhibited anisometric shape with average length and width equal to 90 and 76 nm, respectively, and an aspect ratio of 1.2. The solubility limits of ytterbium and erbium codoped in the CaFCl host were estimated to be \approx 0.60 and 0.09 mol. %, respectively. Green emissions and luminescence decays from the $^2H_{11/2}$ and $^4S_{3/2}$ thermally coupled levels of Er $^{3+}$ were analyzed from the perspective of using CaFCl:Yb,Er for optical temperature sensing. When operating as a ratiometric thermometer, a maximum temperature sensitivity of $3.4 \times 10^{-2} \, \text{K}^{-1}$ was obtained at 150 K. Much lower sensitivities were computed when nanocrystals were used a lifetime thermometer, with a maximum of $2.0 \times 10^{-3} \, \text{K}^{-1}$ at 275 K. Analysis of luminescence decays revealed the presence of a single type of Er $^{3+}$ activator. Radiative constants of the $^2H_{11/2}$ and $^4S_{3/2}$ levels and activation energy for thermal quenching of the latter were estimated.

1. Introduction

Owing to their ability to incorporate optically active dopants such as rare-earth (Nd $^{3+}$, Sm $^{2+/3+}$, Eu $^{2+/3+}$, Gd $^{3+}$, Er $^{3+}$, Tm $^{2+/3+}$, Yb $^{2+/3+}$) [1-18] and transition metals (Mn²⁺) [1], alkaline-earth fluorohalides have been used as host materials to produce X-ray storage phosphors and down- and upconverting phosphors. This family of mixed-halides features MFX as chemical formula (M = Ca, Sr, Ba; X = Cl, Br, I) and is comprised of eight isostructural members obtained via isovalent substitutions of the alkaline-earth metal and of the heavy halogen. Isovalent substitutions in the host lattice enable gradual tuning of crystal-chemical features directly involved in the luminescence response of the activators; these features include vibrational energies [19-23], dimensionality of the metal sublattice [24-28], and local environment of metal atoms [24,29,30]. Altogether, chemical and structural tunability make alkaline-earth fluorohalides an ideal platform to probe the interplay between crystal-chemistry and luminescence. In order to further understand this interplay and develop novel optical materials, our group has been working on the synthesis, structural elucidation, and characterization of the luminescence response of alkaline-earth fluorohalide nanocrystals doped with rare-earth metals [14,17,31,32]. NIR-to-visible upconverting nanocrystals doped with Yb³⁺-Er³⁺

sensitizer—activator pairs are the focus of our research. One of the specific aims we are pursuing is to establish their temperature-dependent luminescence with an eye towards optical thermometry, as a part of a continuous effort to expand the library of materials capable of serving as luminescence thermometers. In this regard, the potential of rare-earth-doped alkaline-earth fluorohalides remains underexplored.

As a follow-up of our studies on SrFCl:Yb,Er and SrFBr:Yb,Er [32], herein we report the synthesis of CaFCl:Yb,Er upconverting nanocrystals and an investigation of their luminescence response in the 150-450 K temperature range. A series of nanocrystals doped with increasing concentrations of Yb³⁺ and Er³⁺ is synthesized by decomposing metal trifluoroacetates and thrichloroacetic acid in a mixture of high-boiling point organic solvents. The chemical composition and morphology of the resulting nanocrystals are established using a combination of X-ray diffraction, elemental analysis, and transmission electron microscopy. Steady-state and time-resolved luminescence studies are performed to establish the potential of using green emissions from the ${}^{2}H_{11/2}$ and ${}^{4}S_{3/2}$ thermally coupled levels of Er³⁺ for temperature sensing. Figures-of-merit including temperature sensitivity, accuracy, resolution, and repeatability are computed for CaFCl:Yb,Er operating as a ratiometric thermometer and compared to those reported for other materials, including fluorohalides. Finally, the distribution of Er³⁺ activators in the

E-mail address: far@chem.wayne.edu (F.A. Rabuffetti).

 $^{^{\}ast}$ Corresponding author.

CaFCl host and their photophysics are probed using time-resolved luminescence.

2. Experimental

2.1. Synthesis

Standard Schlenk techniques were used for the synthesis of CaFCl:Yb,Er nanocrystals. CaCO $_3$ (99%), Yb $_2$ O $_3$ (99.9%), Er $_2$ O $_3$ (99.99%), anhydrous CF $_3$ COOH (99%), oleic acid (90%), and 1-octadecene (90%) were purchased from Sigma-Aldrich and used as received. CCl $_3$ COOH (99%) was purchased from Alfa Aesar and stored in a nitrogen-filled glovebox (oxygen and water levels below 1 ppm).

Metal Trifluoroacetate Precursors. CaFCl:Yb,Er nanocrystals with nominal total rare-earth concentrations (Ca:Yb:Er molar ratios) of 0.25 (2.9925:0.00675:0.00075),0.50 0.75 (2.985:0.0135:0.0015), (2.9700:0.0270:0.0030), (2.9775:0.02025:0.00225),1.00 and 2.00 mol. % (2.9400:0.0540:0.0060) were synthesized using metal trifluoroacetates as starting materials. Trifluoroacetates were prepared by adding stoichiometric amounts of CaCO₃, Yb₂O₃, and Er₂O₃ to a 50 mL two-neck round-bottom flask containing 5 mL of double-deionized water and 1 mL of CF₃COOH. Then, the flask was immersed in a sand bath at 65 °C and heated for 12 h to obtain a colorless, optically transparent solution. The total metal content of the resulting solution was 3 mmol and the nominal erbium concentration was fixed at 10.0% of the total rare-earth concentration (i.e., Yb:Er molar ratio equal to 9). Polycrystalline precursors were obtained after solvent evaporation at 65 °C for 48 h under a constant flow of nitrogen (200 mL min⁻¹) [33]. The resulting solids were kept under static nitrogen atmosphere.

CaFCl:Yb,Er Nanocrystals. Nanocrystals were synthesized via twostep solution thermolysis [8,14]. In the first step, a mixture of oleic acid (10 mL) and 1-octadecene (14 mL) was added to the trifluoroacetate precursor in a two-neck flask. The flask was immersed in a sand bath and heated at 115 °C for 1 h under vacuum (\approx 1 mTorr) with vigorous magnetic stirring. Then, the atmosphere was switched to nitrogen and a needle thermocouple was placed inside the flask in direct contact with the solution. The temperature was increased to 250 °C and, after 1 h, the flask was removed from the sand bath and allowed to cool to room temperature. CaF2:Yb,Er colloidal nanocrystals were thus obtained. In the second step, CCl₃COOH (1 mmol) was weighed inside a glovebox and quickly added to the solution containing CaF2:Yb,Er nanocrystals. Magnetic stirring was used for 10 min to aid in the dissolution of CCl₃COOH. Once CCl₃COOH was fully dissolved, the flask was immersed in a sand bath and heated at 130 °C for 1 h under vacuum (≈1 mTorr) with vigorous magnetic stirring. Then, the atmosphere was switched to nitrogen and a needle thermocouple was placed inside the flask in direct contact with the solution. The temperature was increased to 265 °C and, after 40 min, the flask was removed from the sand bath and quenched to room temperature using a stream of air. A light yellow turbid solution was obtained. CaFCl:Yb,Er nanocrystals were recovered using ethanol followed by centrifugation at 8000 rpm for 10 min. The resulting supernatant was discarded and the precipitate was resuspended in 5 mL toluene and reprecipitated using a mixture of 7 mL of ethanol and 2 mL of methanol. The suspension was centrifuged at 8000 rpm for 10 min. Finally, the resulting precipitate was dried in vacuum at room temperature for 12 h to yield an off-white solid that was used for chemical, morphological, and luminescence studies. Solids, which consisted of CaFCl:Yb,Er nanocrystals, were stored in the glovebox due to their very high sensitivity towards atmospheric moisture.

2.2. Powder X-ray diffraction (PXRD)

PXRD patterns were collected at room temperature using a Bruker D2 Phaser operated at 30 kV and 10 mA. Cu K α radiation ($\lambda=1.5418$ Å) was employed. A nickel filter was utilized to remove Cu K β . Diffractograms were collected in the 10– 60° 2θ range using a step size of 0.025° and a

step time of 0.5 s. Diffractograms for Rietveld analyses were collected in the $10-70^{\circ}$ 2θ range using a step size of 0.0125° and a step time of 0.7 s.

2.3. Rietveld analysis

Rietveld analysis [34,35] of PXRD patterns was performed using the General Structural System (GSAS) with the graphical user interphase (EXPGUI) software [36,37]. The crystal structure of CaFCl:Yb,Er was refined using the tetragonal P4/nmm space group. The following parameters were refined: (1) scale factor; (2) background, which was modeled using a shifted Chebyshev polynomial function; (3) peak shape, which was modeled using a modified Thompson–Cox–Hasting pseudo-Voight function; [38] (4) lattice constants (a and c); (5) fractional atomic coordinates of the metal (zM) and chlorine (zCl) atoms; and (6) an isotropic displacement parameter for each chemically distinct atom (U_{M} , U_{F} , U_{Cl}). The occupancy of the metal site (M) was fixed according to the Ca:Yb:Er ratios obtained from elemental analysis. Visual inspection of the difference curves and R_{wp} residual values were used to assess the quality of the refinements.

2.4. Transmission electron microscopy imaging (TEM)

TEM images were obtained using a JEOL JEM2010F (JEOL Ltd.) electron microscope operated at 200 kV. Specimens were prepared by mixing the colloidal solution containing CaFCl:Yb,Er nanocrystals with toluene and dropcasting this mixture on a 200 mesh copper grid coated with a Lacey carbon film (Ted Pella Inc.). Size distribution histograms were obtained after analyzing 300 nanocrystals.

2.5. Inductively coupled plasma mass spectrometry (ICP-MS)

Elemental analyses of metals in CaFCl:Yb,Er nanocrystals were carried out using a 7700 Series ICP–MS (Agilent Technologies). $\approx 3-4\,mg$ of sample were dissolved in 20 mL of aqua regia at room temperature. Ytterbium (1000 μg mL $^{-1}$, High Purity Standards), erbium (998 \pm 4 μg mL $^{-1}$, Fluka), and calcium (1000 μg mL $^{-1}$, High Purity Standards) in 2% HNO3 were used as standards.

2.6. Spectrofluorometry

Spectrofluorometric analyses were conducted using a Fluorolog 3-222 fluorometer (Horiba Scientific). Steady-state spectra were collected using a MDL-N-980 (Opto Engine, LLC) continuous-wave 980 nm laser as the excitation source and a photomultiplier tube R928 as the detector. Luminescence decays were recorded by operating the laser in pulsed mode. Spectra and decays were collected at room temperature for all five members of the CaFCl:Yb,Er series synthesized in this work. Variable-temperature measurements were performed for CaFCl:Yb,Er nanocrystals featuring a nominal total rare-earth concentration of 2.00 mol. %. For this sample, a 5% (w/w) CaFCl:Yb,Er/BaSO₄ mixture was prepared inside the glove box (BaSO₄, 99.9%, Sigma Aldrich). This mixture was loaded into a VPF-800 variable-temperature stage (Janis Research Company) and degassed under vacuum (≈100 mTorr) at 400 K for 2 h and at room temperature for 12 h prior to data collection. Temperature was set by a Lake Shore 335-3060 controller (Lake Shore Cryotronics). Emission spectra and luminescence decays were collected in the 150-450 K temperature range at 25 K intervals. A heating rate of 5 K min⁻¹ was employed. Samples were allowed to dwell for \approx 10 min at the target temperature prior to data collection. Spectra were recorded between 500 and 700 nm using a slit width of 2 nm. An excitation power density of $\approx 2.0~\text{W}~\text{cm}^{-2}$ was used unless indicated otherwise.

3. Results and discussion

The phase purity, elemental composition, and morphology of CaFCl:

Yb,Er nanocrystals were probed using PXRD, ICP-MS, and TEM, respectively. Results from these analyses are summarized in Fig. 1. A representative Rietveld refinement is shown in Fig. 1a for the case of nanocrystals doped with 2.00 mol. %. Structural parameters extracted from this refinement are given in the Supporting Information along with PXRD patterns for other compositions (Table S1 and Fig. S1). Inspection of the difference curve confirmed the phase purity of the nanocrystals; all diffraction maxima were indexed to the fluorochloride phase (PDF No. 01–070–0483, a = 3.8884(2) Å, c = 6.8471(6) Å). No maxima corresponding to secondary crystalline phases were observed. Incorporation of rare-earth ions in the nanocrystals was confirmed by ICP-MS elemental analyses. Fig. 1b shows the experimentally determined concentrations of rare-earth metals as a function of their nominal values; numeric values are given in the Supporting Information (Table S2). An increase in the total rare-earth concentration was observed upon increasing the nominal concentration, followed by saturation at ≈ 0.70 mol. %. Similar trends were encountered for the concentrations of vtterbium and erbium; for the former, the solubility limit appeared at \approx 0.60 mol. % and for the latter at \approx 0.09 mol. %. These values are significantly smaller than those reported for ytterbium and erbium codoped into SrFCl and BaFCl colloidal nanocrystals [14], indicating the much lower solubility of these rare-earths in CaFCl. Erbium represented between 9.0 and 12% of the total rare-earth content in the nanocrystals, in good agreement with the target value of 10%. Electroneutrality requires that incorporation of rare-earth dopants is accompanied by the formation of charge-compensating defects. Pure and aliovalently doped single crystal and bulk alkaline-earth fluorohalides have been shown to incorporate oxide anions as defects or as charge-compensating species [39–42]. This may also be the case in CaFCl:Yb,Er nanocrystals, as oxygen traces were certainly present in the reaction medium. Finally, TEM imaging revealed that nanocrystals exhibited nonisometric shape. As shown in Fig. 1c, their average edge length and width were 90 and 76 nm, respectively, yielding an average aspect ratio of 1.2. TEM images and size distribution histograms corresponding to other compositions are given in the Supporting Information (Fig. S2). The nanocrystals' morphology was found to be independent of the rare-earth concentration.

The ability of CaFCl:Yb,Er nanocrystals to perform NIR-to-visible upconversion at room temperature was probed prior to investigating their temperature-dependent luminescence. Fig. 2 provides a representative emission spectrum and luminescence decays corresponding to nanocrystals doped with a total rare-earth concentration of 2.00 mol. %.

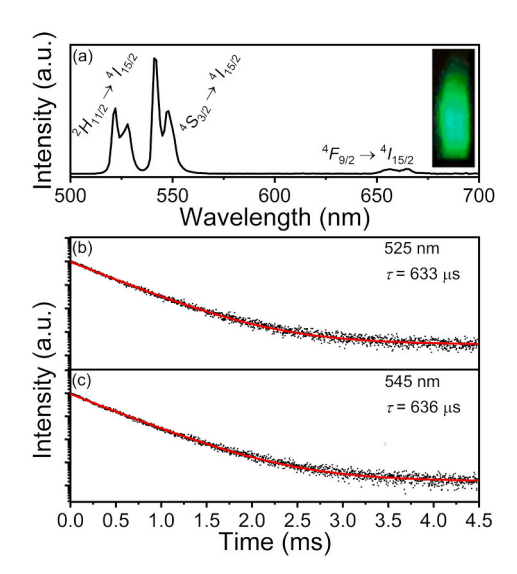


Fig. 2. (a) Room-temperature emission spectrum of CaFCl:Yb,Er nanocrystals (2.00 mol. %) under 980 nm excitation. A digital picture of the phosphor under NIR light is shown in the inset. (b, c) Luminescence decays of the $^2H_{11/2}$ (525 nm) and $^4S_{3/2}$ (545 nm) excited states of Er $^{3+}$. Monoexponential fits are depicted as solid red lines and the corresponding lifetimes (τ) are indicated.

Emission spectra and decays for other compositions are given in the Supporting Information (Figs. S3 and S4). As shown in Fig. 2a, emission spectra were dominated by two green bands centered at $\approx\!525$ and 545 nm; these bands were assigned to the $^2H_{11/2} \to ^4I_{15/2}$ and $^4S_{3/2} \to ^4I_{15/2}$ f–f transitions of the ${\rm Er}^{3+}$ activator, respectively. In addition, a much weaker red band corresponding to the $^4F_{9/2} \to ^4I_{15/2}$ transition was observed at $\approx\!660$ nm. As a consequence of this spectral distribution, CaFCl:Yb,Er behaved as a green phosphor under 980 nm excitation. This result was found to be independent of the rare-earth concentration, although the intensity of green bands increased with doping level. The excited-state lifetimes of the ${\rm Er}^{3+}$ activator(s) (τ) were extracted by fitting luminescence decays at 525 and 545 nm with a monoexponential function (Eq. (1), where I(t) is intensity at time t, and α and β are constants).

$$I(t) = \alpha \exp(-t/\tau) + \beta \tag{1}$$

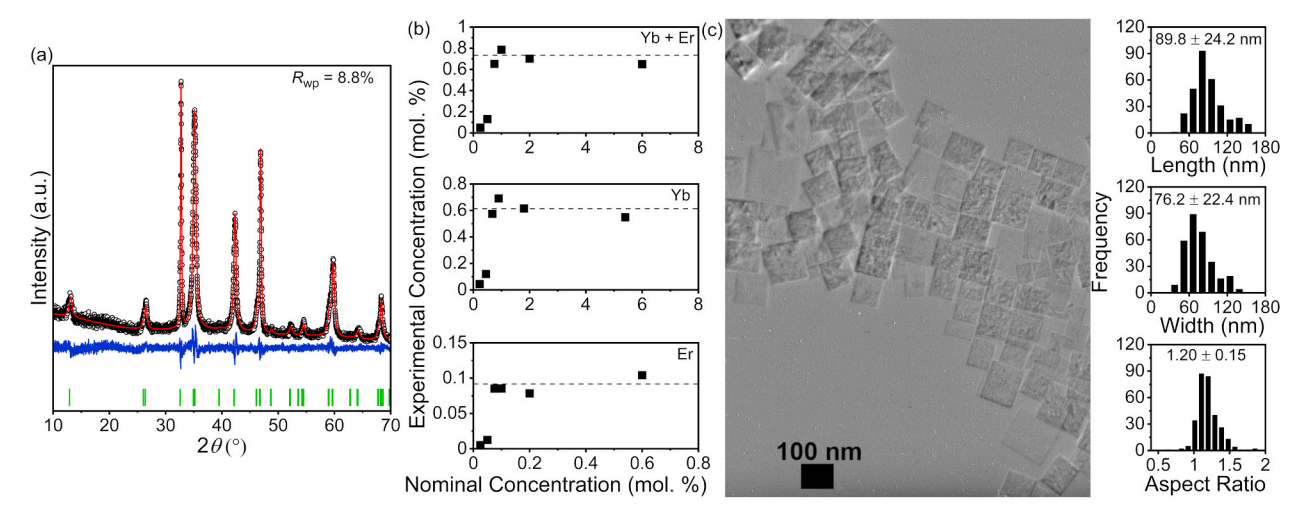


Fig. 1. (a) Rietveld analysis of the PXRD pattern of CaFCl:Yb,Er nanocrystals (2.00 mol. %). Experimental (hollow black circles) and calculated patterns (solid red line), difference curve (solid blue line), and tick marks (vertical green bars) corresponding to the calculated position of the diffraction maxima are given. (b) Experimentally determined rare-earth concentrations as a function of their nominal values. Total (Yb + Er), ytterbium (Yb), and erbium (Er) concentrations are shown. Dashed lines indicate estimated solubility limits. (c) TEM image of CaFCl:Yb,Er nanocrystals and histograms illustrating the distribution of lengths, widths, and aspect ratios.

As shown in Fig. 2b and c, lifetimes of 633 and 636 μ s were obtained for $^2H_{11/2}$ and $^4S_{3/2}$, respectively; values in the 440–601 and 436–610 μ s ranges were obtained for other compositions. From the standpoint of the distribution of ${\rm Er}^{3+}$ activators within the CaFCl lattice, the observation of a monoexponential decay reflected the presence of a single emitting center. This result is qualitatively different from what was reported for ${\rm Er}^{3+}$ doped into SrFCl, SrFBr, and BaFCl nanocrystals, in which luminescence decays were found to be biexponential [14,17,31,32].

The temperature-dependent luminescence of CaFCl:Yb,Er nanocrystals was probed with the aim of exploring their potential as ratiometric thermometers. Emission spectra were collected between 150 and 450 K for nanocrystals featuring a total rare-earth concentration of 2.00 mol. %. The choice of this composition was based on the observation that it displayed the most intense green emission at room temperature. Results from these studies are summarized in Fig. 3. Fig. 3a depicts the evolution with temperature of the two green emission bands centered at 525 and 545 nm. As expected for a pair of thermally coupled levels such as ${}^{2}H_{11/2}$ and ${}^{4}S_{3/2}$, the intensity of the upper level (${}^{2}H_{11/2}$) increased with temperature while that of the lower level (${}^4S_{3/2}$) decreased. This trend was also reflected in the integrated intensities of the two emission bands, which are plotted in Fig. 3b. Integrated intensities were used to calculate the luminescence intensity ratio (R(T), Eq. (2)) and derive temperature sensitivity ($S_R(T)$, Eq. (3)). R(T) values were fit with a modified Boltzmann's distribution (Eq. (4)) [43].

$$R(T) = \frac{I({}^{2}H_{11/2} \to {}^{4}I_{15/2})}{I({}^{4}S_{3/2} \to {}^{4}I_{15/2})}$$
(2)

$$S_R(T) = \frac{1}{R(T)} \frac{dR(T)}{dT} \tag{3}$$

$$R(T) = A \exp\left(-\frac{\Delta E}{k_B T}\right) + B \tag{4}$$

In Eq. (4), A and B are constants, ΔE is the energy gap between the ${}^2H_{11/2}$ and ${}^4S_{3/2}$ levels, $k_{\rm B}$ is Boltzmann's constant, and T is the absolute temperature. As shown in Fig. 3c, a good fit was obtained using A = 13.84(18), $\Delta E = 625(4) \text{ cm}^{-1}$, and $B = 5.9(4.2) \times 10^{-3}$ as adjustable parameters. The ${}^{2}H_{11/2}$ -to- ${}^{4}S_{3/2}$ energy gap extracted from the fit (625 cm⁻¹) was comparable to the value obtained from the emission spectra (693 cm⁻¹, see Fig. S5 in the Supporting Information). Temperature sensitivity values plotted in Fig. 3d dropped from a maximum of $3.4 \times 10^{-2} \text{ K}^{-1}$ at 150 K to a minimum of $4.4 \times 10^{-3} \text{ K}^{-1}$ at 450 K. Inspection of these values revealed the potential of CaFCl:Yb,Er nanocrystals as optical thermometers for low temperature regimes. Indeed, their sensitivity at 150 K is in the middle of the range of values reported for other erbium-activated upconverting nanothermometers at the same temperature; examples include SrFCl:Yb,Er $(2.6 \times 10^{-2} \text{ K}^{-1})$ [32], SrFBr:Yb,Er $(1.6 \times 10^{-2} \text{ K}^{-1})$ [32], NaGdF₄:Yb,Er $(4.5 \times 10^{-2} \text{ K}^{-1})$ [44], and Y_2O_3 :Yb,Er (5.3 \times 10⁻² K⁻¹) [45]. On this basis, we evaluated the repeatability, temperature accuracy, and temperature resolution of CaFCl:Yb,Er nanocrystals at 150 K to further assess their potential as luminescence thermometers. Repeatability was computed by subjecting nanocrystals to 10 heating-cooling cycles and extracting luminescence intensity ratios (Eq. (5)).

Repeatability(T) =
$$100 \times \left(1 - \frac{max|R_i(T) - \langle R(T) \rangle|}{\langle R(T) \rangle}\right)$$
 (5)

Here, $R_i(T)$ is the value of the ratio in the ith cycle and $\langle R(T) \rangle$ is the mean value of the ratio computed over 10 cycles. Emission spectra collected during these cycles were used to estimate temperature accuracy

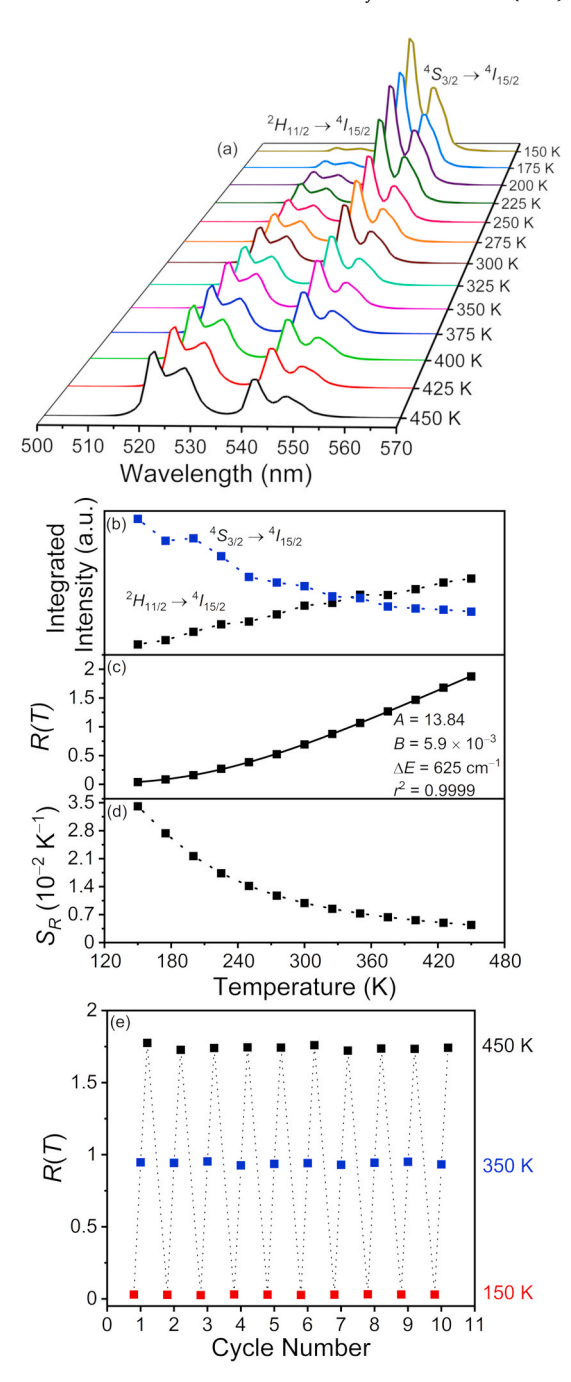


Fig. 3. (a) Temperature-dependent emission spectra of CaFCl:Yb,Er nanocrystals (2.00 mol. %) under 980 nm excitation. Integrated intensities of the green emission bands (b), luminescence intensity ratio R(T) (c), and temperature sensitivity $S_R(T)$ (d) as a function of temperature. Fit of Eq. (4) to R(T) is depicted as a solid line in (c). Parameters extracted from the fit and fit residual r^2 are given. (e) Luminescence intensity ratio as a function of the heating-cooling cycle. Dotted lines in (b), (d), and (e) are guides-to-the-eye.

 $(\langle T_{calculated} \rangle)$ and resolution (ΔT) as the mean and standard deviation of the calculated temperature values, respectively. Results from repeatability tests are plotted in Fig. 3e; numeric data are given in the Supporting Information (Table S3). The repeatability, mean calculated temperature, and temperature resolution of CaFCl:Yb,Er nanocrystals at 150 K were found to be 91%, 140.9 K, and 1.6 K, respectively.

Comparable values were obtained at higher temperatures (99%, 333.6 K, and 1.2 K at 350 K; 98%, 433.2 K, and 1.9 K at 450 K). We attribute the systematic underestimation of temperature to the high sensitivity of the nanocrystals towards moisture coupled to exposure to air when loading the sample into the variable-temperature stage.

Finally, we investigated the potential of CaFCl:Yb,Er as a lifetime nanothermometer. To this end, luminescence decays of the $^2H_{11/2}$ and $^4S_{3/2}$ thermally coupled excited levels of ${\rm Er}^{3+}$ were collected between 150 and 450 K for nanocrystals featuring a total rare-earth concentration of 2.00 mol. %. Lifetimes were extracted via monoexponential fits and, once in hand, their temperature-dependence was fit considering (1) thermal equilibrium between the $^2H_{11/2}$ and $^4S_{3/2}$ levels [46–48], and (2) the presence of a temperature-dependent nonradiative energy-transfer pathway in addition to thermalization (Eq. (6)).

$$\tau_{4_{S_{3/2}}}(T) = \left(\frac{k_R^{4_{S_{3/2}}} + 3k_R^{2_{H_{11/2}}} exp^{-\frac{\Delta E}{k_B T}}}{1 + 3 exp^{-\frac{\Delta E}{k_B T}}} + k_{ET} exp^{-\frac{E_g}{k_B T}}\right)^{-1}$$
(6)

In Eq. (6), $k_R^{4s_{3/2}}$ and $k_R^{2H_{11/2}}$ are the radiative constants of the ${}^4S_{3/2}$ and ${}^{2}H_{11/2}$ levels, respectively, ΔE is the energy gap between them, k_{ET} is an energy-transfer rate constant, and E_a is the activation energy for energy transfer. The contribution of multiphonon relaxation to the decay of the $^{2}H_{11/2}/^{4}S_{3/2}$ manifold was negligible in the 100–450 K temperature range due to the large energy gap between the ${}^4S_{3/2}$ and ${}^4F_{9/2}$ levels $(\approx 3215 \text{ cm}^{-1}, \text{ see Supporting Information, Fig. S5})$ and the low energy of the vibrational modes of the CaFCl host (≈336 cm⁻¹) [49]. Results from time-resolved studies are summarized in Fig. 4; decay curves and lifetimes extracted from monoexponential fits are provided in the Supporting Information (Fig. S6 and Table S4). As shown in Fig. 4a, a good fit was obtained using $k_R^{4s_{3/2}}=1106(12)~{\rm s}^{-1},~k_R^{2H_{11/2}}=1406(886)~{\rm s}^{-1},~k_{ET}=3642(1114)~{\rm s}^{-1},~{\rm and}~E_a=505(24)~{\rm cm}^{-1}$ as adjustable parameters (ΔE was fixed at 693 cm⁻¹). To the best of our knowledge, radiative constants of the green emissive levels of Er³⁺ doped into CaFCl have not been reported. Values provided in this work are comparable to those computed for Er^{3+} doped into CaF_2 (${}^4S_{3/2}$: 1770–2809 s^{-1} ; ${}^2H_{11/2}$: 1703–2512 s⁻¹) [50,51] and into other fluorohalides such as SrFBr $(^4S_{3/2}: 1801 \text{ s}^{-1})$ [32]. In addition, the magnitude of the activation energy is consistent with nonradiative energy-transfer processes that depopulate the ${}^4S_{3/2}$ level. A phonon-assisted cross-relaxation of the type ${}^4S_{3/2}$, ${}^4I_{15/2} \rightarrow {}^4I_{9/2}$, ${}^4I_{13/2}$ may be responsible for the observed thermal quenching, similar to what was reported by Ryba-Romanowski for Er³⁺-doped tellurite glasses [46]. He found this nonradiative energy-transfer pathway to be operative between 145 and 500 K and activation energy of 467 cm^{-1} . temperature-dependent lifetimes of the ${}^4S_{3/2}$ level were used to estimate the sensitivity of CaFCl:Yb,Er nanocrystals as a lifetime thermometer

$$S_{\tau}(T) = \frac{1}{\tau(T)} \frac{d\tau(T)}{dT} \tag{7}$$

Fig. 4b shows that the sensitivity reached a maximum of $2.0 \times 10^{-3}~{\rm K}^{-1}$ at 275 K. More importantly, sensitivity values obtained while operating as a lifetime thermometer were significantly smaller than those achieved in ratiometric mode. This result, valid within the entire temperature range studied in this work, favors the usage of CaFCl:Yb,Er nanocrystals as a ratiometric thermometer.

4. Conclusions

In conclusion, the solution-phase synthesis of CaFCl:Yb,Er upconverting nanocrystals was described and their luminescence probed in the $100-450\,$ K temperature range. Solubility limits for codoping

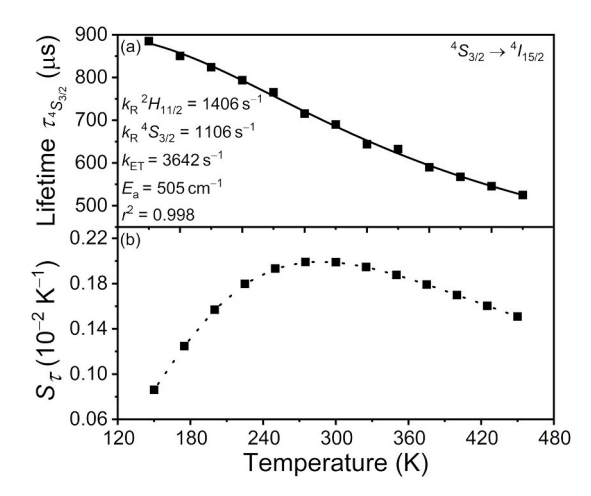


Fig. 4. (a) Lifetime of the ${}^4S_{3/2}$ excited state of Er $^{3+}$ in CaFCl:Yb,Er nanocrystals (2.00 mol. %) as a function of temperature. Fit of Eq. (6) to the temperature-dependent lifetime of the ${}^4S_{3/2}$ level is depicted as a solid line. Parameters extracted from the fit and fit residual r^2 are given. (b) Temperature sensitivity $S_r(T)$ as a function of temperature. The dotted line is a guide-to-the-eye

Yb³⁺-Er³⁺ sensitizer-activator pairs into CaFCl were established and the ability of the nanocrystals to serve as green upconverting phosphors was demonstrated. Their potential as ratiometric and lifetime thermometers was quantitatively assessed. In the case of CaFCl:Yb,Er nanocrystals operating as a ratiometric thermometer, a comprehensive evaluation of temperature sensitivity, accuracy, resolution, and repeatability was carried out. A maximum sensitivity of $3.4 \times 10^{-2} \, \text{K}^{-1}$ was estimated at 150 K. This value was comparable to that reported for other nanomaterials used as erbium-activated upconverting thermometers for low temperatures, and significantly higher than those obtained when the nanocrystals operated as lifetime thermometers. Finally, radiative constants of the ${}^2H_{11/2}$ and ${}^4S_{3/2}$ levels of ${\rm Er}^{3+}$ doped into CaFCl were extracted from temperature-dependent decays. Moving forward, chemical stability appears to be the major obstacle to further develop CaFCl:Yb,Er nanocrystals as optical temperature sensors. Synthetic work is underway to address and mitigate their sensitivity toward moisture.

Declaration of competing interest

The authors declare that they have no known competing financial interests or personal relationships that could have appeared to influence the work reported in this paper.

Acknowledgements

D.B. was supported by the National Science Foundation (DMR-2003118). H.N.M was supported through a Thomas C. Rumble Graduate Fellowship. F. A. R. would like to acknowledge the support of the Research Corporation for Science Advancement through a Cottrell Scholar Award. The authors are grateful for the support of the Department of Chemistry at Wayne State University and for the use of the X-ray core in the Lumigen Instrument Center (National Science Foundation, MRI-1427926).

Appendix A. Supplementary data

Supplementary data to this article can be found online at https://doi.org/10.1016/j.jlumin.2021.117974.

References

- [1] D. Zevenhuijzen, J.A. Vanwinsum, H.W.D. Hartog, S-state ions in tetragonal SrFCl, J. Phys. Chem. 9 (1976) 3113–3119.
- [2] K. Takahashi, J. Miyahara, Y. Shibahara, Photostimulated luminescence (PSL) and color-centers in BaFCl-Eu²⁺, BaFBr-Eu²⁺, BaFI-Eu²⁺ phosphors, J. Electrochem. Soc. 132 (1985) 1492–1494.
- W.J. Schipper, G. Blasse, Luminescence of ytterbium(II) in alkaline-earth [3] fluorohalides, J. Solid State Chem. 94 (1991) 418-427.
- [4] R.J. Klee, An X-ray diffraction study of (Ba,Sr)F_{1+x}Br_{1-x}:Eu²⁺, a new X-ray image receptor, Material. J. Phys. D 28 (1995) 2529–2533.
- X.Y. Chen, G.K. Liu, The standard and anomalous crystal-field spectra of Eu³⁺. J. Solid State Chem. 178 (2005) 419-428.
- [6] H. Riesen, W.A. Kaczmarek, Efficient X-ray generation of Sm²⁺ in nanocrystalline BaFCl/Sm³⁺: a photoluminescent X-ray storage phosphor, Inorg. Chem. 46 (2007) 7235–7237.
- O. Ju, Y.S. Liu, R.F. Li, L.O. Liu, W.O. Luo, X.Y. Chen, Optical spectroscopy of Eu³⁺doped BaFCl nanocrystals, J. Phys. Chem. C 113 (2009) 2309-2315.
- [8] D. Chen, Y. Yu, F. Huang, P. Huang, A. Yang, Z. Wang, Y. Wang, Monodisperse upconversion Er³⁺/Yb³⁺:MFCl (M = Ca, Sr, Ba) nanocrystals synthesized via a seed-based chlorination route, Chem. Commun. 47 (2011) 11083-11085.
- [9] Z.O. Liu, M. Stevens-Kalceff, H. Riesen, Photolyminescence and cathodoluminescence properties of nanocrystalline BaFCl:Sm³⁺ X-ray storage phosphor, J. Phys. Chem. C 116 (2012) 8322–8331.
- [10] P. Pal, T. Penhouet, V. D'Anna, H. Hagemann, Effect of temperature and pressure on emission lifetime of Sm^{2+} ion doped in MFX (M = Sr, Ba; X = Br, I) crystals, J. Lumin, 142 (2013) 66-74.
- [11] X.-L. Wang, Z.-Q. Liu, M. Stevens-Kalceff, H. Riesen, Mechanochemical preparation of nanocrystalline BaFCl doped with samarium in the 2+ oxidation state, Inorg Chem. 53 (2014) 8839-8841.
- [12] J. Zhang, H. Riesen, Controlled generation of Tm²⁺ ions in nanocrystalline BaFCl: Tm³⁺ by X-ray irradiation, J. Phys. Chem. 121 (2017) 803–809.
- [13] J. Zhang, N. Riesen, H. Riesen, Mechanochemically prepared SrFCl nanophosphor codoped with Yb^{3+} and Er^{3+} for detecting ionizing radiation by upconversion luminescence, Nanoscale 9 (2017) 15958–15966.
- [14] K.T. Dissanayake, F.A. Rabuffetti, Multicolor emission in chemically and structurally tunable Er:Yb:SrFX (X = Cl, Br) upconverting nanocrystals, Chem. Mater. 30 (7) (2018) 2453-2462.
- [15] J. Wei, W. Lian, W. Zheng, X. Shang, M. Zhang, T. Dai, X. Chen, Sub-10 nm lanthanide-doped SrFCl nanoprobes: controlled synthesis, optical properties, and bioimaging, J. Rare Earths 37 (2019) 691-698.
- [16] J. Zhang, H. Riesen, Photostimulated and persistent luminescence of samarium ions in BaFCl, J. Lumin. 207 (2019) 188-194.
- [17] K.T. Dissanayake, D.K. Amarasinghe, L. Suescun, F.A. Rabuffetti, Accessing mixedhalide upconverters using heterohaloacetate precursors, Chem. Mater. 31 (2019) 6262-6267.
- [18] X. Zhao, Q. Yu, J. Yuan, N.V. Thakor, M.C. Tan, Biodegradable rare earth fluorochloride nanocrystals for phototheranostics, RSC Adv. 10 (2020) 15387-15393
- [19] J.F. Scott, Raman spectra of BaClF, BaBrF, and SrClF, J. Chem. Phys. 49 (1968) 2766-2769.
- [20] H.L. Bhat, M.R. Srinivasan, S.R. Girisha, A.H.R. Rao, P.S. Narayanan, Growth and infrared spectra of some mixed dihalides, Indian J. Pure Appl. Phys. 15 (1977)
- [21] K.R. Balasubramanian, T.M. Haridasan, Lattice dynamics of BaClF and SrFCl, J. Phys. Chem. Solid. 42 (1981) 667-675.
- M. Sieskind, D. Ayachour, J.C. Merle, J.C. Boulou, Crystal growth, Raman, and infrared spectra of BaFI single crystals, Phys. Status Solidi B 158 (1990) 103-112.
- [23] R. Mittal, S.L. Chaplot, A. Sen, S.N. Achary, A.K. Tyagi, Lattice dynamics and inelastic neutron scattering studies of MFX (M = Ba, Sr, Pb; X = Cl, Br, I), Phys. Rev. B 67 (2003) 134303.
- [24] H.P. Beck, Study on mixed halide compounds MFX (M = Ca, Sr, Ba; X = Cl, Br, I), J. Solid State Chem. 17 (1976) 275-282.

- [25] Y.R. Shen, U. Englisch, L. Chudinovskikh, F. Porsch, R. Haberkorn, H.P. Beck, W. B. Holzapfel, A structural study on the PbFCl-type compounds MFCl (M = Ba, Sr, and Ca) and BaFBr under high-pressure, J. Phys. Condens. Matter 6 (1994)
- [26] F. Decremps, M. Fischer, A. Polian, J.P. Itie, M. Sieskind, Ionic layered PbFCl-type compounds under high pressure, Phys. Rev. B 59 (1999) 4011-4022.
- F. Decremps, M. Fischer, A. Polian, J.P. Itie, M. Sieskind, Prediction of cell variations with pressure of ionic layered crystal. Application to the matlockite family, Eur. Phys. J. B 9 (1999) 49-57.
- [28] M. Sieskind, J. Morel, Structural considerations and polarization energy of some PbFCl-type compounds, J. Solid State Chem. 144 (1999) 339-348.
- [29] B.W. Liebich, D. Nicollin, Refinement of PbFCl types BaFI, BaFBr, and CaFCl, Acta Crystallogr. B 33 (1977) 2790-2794.
- [30] M. Sauvage, Refinement of structures of SrFCl and BaFCl, Acta Crystallogr. B 30 (1974) 2786-2787.
- [31] K.T. Dissanayake, F.A. Rabuffetti, Infrared-to-visible upconversion luminescence in Er:Yb:SrFBr nanocrystals, J. Mater. Chem. C 4 (2016) 2447–2451.
- [32] S.S. Perera, K.T. Dissanayake, F.A. Rabuffetti, Alkaline-earth fluorohalide nanocrystals for upconversion thermometry, J. Lumin. 207 (2019) 416-423.
- [33] K.T. Dissanayake, L.M. Mendoza, P.D. Martin, L. Suescun, F.A. Rabuffetti, Openframework structures of anhydrous Sr(CF3COO)2 and Ba(CF3COO)2, Inorg. Chem. 55 (2016) 170-176.
- [34] H.M. Rietveld, Line profiles of neutron powder-diffraction peaks for structure refinement, Acta Crystallogr. 22 (1967) 151-152.
- [35] H.M. Rietveld, A profile refinement method for nuclear and magnetic structures, J. Appl. Crystallogr. 2 (1969) 65-71.
- A.C. Larson, R.B. Von Dreele, General Structure Analysis System (GSAS), Los Alamos National Laboratory, 2000.
- [37] B.H. Toby, EXPGUI, a graphical user interface for GSAS, J. Appl. Crystallogr. 34 (2001) 210-213.
- P. Thompson, D.E. Cox, J.B. Hastings, Rietveld refinement of Debye-Scherrer synchrotron X-ray data from Al₂O₃, J. Appl. Crystallogr. 20 (1987) 79–83.
- C.R.A. Catlow, Oxygen incorporation in the alkaline-earth fluorohalides, J. Phys. Chem. Solid. 38 (1977) 1131-1136.
- E. Radzhabov, V. Otroshok, Optical spectra of oxygen defects in BaFCl and BaFBr crystals, J. Phys. Chem. Solid. 56 (1995) 1-7.
- X.Y. Chen, W. Zhao, R.E. Cook, G.K. Liu, Anomalous luminescence dynamics of Eu³ in BaFCl microcrystals, Phys. Rev. B 70 (2004) 205122.
- Q. Ju, Y.S. Liu, R.F. Li, L.Q. Liu, W.Q. Luo, X.Y. Chen, Optical spectroscopy of Eu³⁺doped BaFCl nanocrystals, J. Phys. Chem. C 113 (2009) 2309-2315.
- S.A. Wade, S.F. Collins, G.W. Baxter, Fluorescence intensity ratio technique for optical fiber point temperature sensing, J. Appl. Phys. 94 (2003) 4743–4756.
- [44] K. Mukhuti, V.N.K.B. Adusumalli, H.V.S.R.M. Koppisetti, B. Bansal, V. Mahalingam, Highly sensitive upconverting nanoplatform for luminescent thermometry from ambient to cryogenic temperature, ChemPhysChem 21 (2020) 1731-1736.
- V. Loipur, G. Nikolić, M.D. Dramićanin, Luminescence thermometry below room temperature via up-conversion emission of Y₂O₃:Yb³⁺,Er³⁺ nanophosphors, J. Appl. Phys. 115 (2014) 203106.
- [46] W. Ryba-Romanowski, Effect of temperature and activator concentration on luminescence decay of erbium-doped tellurite glass, J. Lumin. 46 (1990) 163–172. X. Chen, E. Ma, G. Liu, M. Yin, Excited-state dynamics of ${\rm Er}^{3+}$ in ${\rm Gd}_2{\rm O}_3$
- nanocrystals, J. Phys. Chem. C 111 (2007) 9638-9643.
- [48] J.I. Eldridge, Luminescence decay-based Y2O3:Er phosphor thermometry: temperature sensitivity governed by multiphonon emission with an effective phonon energy transition, J. Lumin. 214 (2019) 116535.
- [49] D. Nicollin, H. Bill, Experimental contribution to the study of S-state ions in ionic single crystals, J. Phys. Chem. 11 (1978) 4803-4814.
- [50] G. Buse, E. Preda, M. Stef, I. Nicoara, Influence of Yb³⁺ ions on the optical properties of double-doped Er,Yb:CaF2 crystals, Phys. Scripta 83 (2011), 025604.
- [51] E. Preda, M. Stef, G. Buse, A. Pruna, I. Nicoara, Concentration dependence of the judd-ofelt parameters of Er³⁺ ions in CaF₂ crystals, Phys. Scripta 79 (2009), 035304